Machine Learning-Based Direction-of-Arrival Estimation Exploiting Distributed Sparse Arrays

Saidur R. Pavel [1], Md. Waqeeb T. S. Chowdhury [1], Yimin D. Zhang [1], Dan Shen [2], and Genshe Chen [2]

[1] Department of Electrical and Computer Engineering, Temple University, Philadelphia, PA 19122, USA
[2] Intelligent Fusion Technology, Inc., Germantown, MD 20876, USA

***Abstract*—Distributed sparse arrays, consisting of multiple subarrays, facilitate a higher number of degrees of freedom and enhanced direction-of-arrival (DOA) estimation performance beyond what is offered by single uniform linear arrays. When the array elements in each subarray are sparsely located, the covariance matrix is sparse with missing entries. Covariance matrix interpolation is commonly exploited to fill in the missing elements of the covariance matrix. Such techniques, however, would degrade or fail when array imperfection occurs, such as imperfect calibration or knowledge in sensor gain, phase, position, and inter-element mutual coupling. Such imperfections affect the matrix interpolation and impede accurate DOA estimation. To address these issues, we propose a neural network structure, which is trained to learn the relationship between the input sparse covariance matrix and the true signal directions. The neural network is trained based on minimizing a loss function between the predicted neural network output and the actual output so that the network is forced to extract the essential feature, rendering accurate DOA estimation results.**

keywords: Distributive array, covariance matrix, MUSIC, neural network, machine learning.

I. Introduction

Direction-of-arrival (DOA) estimation, which determines the spatial spectrum of the impinging electromagnetic or acoustic waves, is one of the fundamental research areas in array signal processing. It finds importance in various applications, including wireless communication, radar, sonar, and astronomical observations [1–3]. A number of methods have been developed for this purpose, such as beamforming techniques [4–6], subspace-based methods [7, 8], sparsity-inducing methods [9–16]. These model-driven methods formulate a parametric mapping from signal direction to array output and assume that the mapping is reversible.

Uniform linear arrays (ULAs) are commonly employed for the DOA estimation [2, 3]. However, they are not efficient in terms of their array aperture, and the degrees of freedom that can be achieved from a ULA is low. A fundamental limitation of ULAs is that we cannot resolve more sources than the number of sensors. To overcome this limitation, a number of studies have been made for detecting more sources than the number of array elements using sparse arrays, particularly through the utilization of their deference co-arrays [17–19]. Minimum redundancy array (MRA) [17] and the minimum hole array (MHA) [18, 20] are well-known classical approaches that utilize the sparse array structure. Recently, systematic sparse array designs, inspired by the nested array [21] and the coprime array [22], are developed to ensure convenient sparse array design and performance analysis [23–27].

When it is infeasible to use an array with many array sensors, distributed array structures become an attractive solution and make it possible to form a large array with multiple low-complexity platforms. Each subarray can either be uniform linear or sparse. Such distributed array formation is desirable and convenient in various applications, including distributive unmanned aerial vehicles (UAVs) and unmanned underwater vehicles (UUVs), where each vehicle is equipped with a small number of antennas or hydrophones.

In this paper, we consider non-coherent data processing at the fusion center, which is practical considering the mobility of the subarrays. In such a platform, each subarray separately computes its individual covariance matrix and sends this information to the fusion center to perform non-coherent processing. All the locally computed covariance matrices are combined together at the fusion center to achieve a higher number of degree of freedom [28]. Improved maneuverability and increased angle measurement accuracy can be achieved by exploiting distributive array structure while maintaining the original array aperture [29].

Non-coherent processing only requires sensor location calibration within each individual subarray, whereas the distance between different subarrays is not required. When sensors are located sparsely in each subarrays, the locally computed covariance matrices are sparse. This generally renders the fused covariance matrix sparse sparse as well with missing values. In this case, when we directly employ conventional subspace-based DOA estimation methods, such as MUSIC, the DOA estimation performance will degrade.

When the fused covariance matrix is sparse, structured matrix completion methods can be utilized to reconstruct missing entries in the covariance matrix [31, 32]. These sophisticated matrix completion methods commonly utilize the Toeplitz and Hermitian structure of the covariance matrix. As a result, such techniques would degrade or fail when array imperfection occurs, such as imperfect calibration or knowledge in sensor gain, phase, position, and inter-sensor mutual coupling. Such imperfections affect the matrix interpolation and impede accurate DOA estimation.

To address such issues, we propose a data-driven approach using neural network for DOA estimation. Machine learning is a well established technique in the field of image, speech, and array signal processing [33–36], and DOA estimation using machine learning techniques is becoming increasingly attractive [37–42]. Machine learning-based DOA estimation is effective to deal with array imperfections in the non-ideal scenario [43, 44]. However, all these studies only consider a small number of sources, and none of them have considered distributed arrays. In contrast to their approaches, we offer a neural network framework for DOA estimation for distributive array, and a high number of sources are handled through effective array information fusion and network training. In the

proposed scheme, sparse covariance matrices locally computed at each subarray is used as the input of the neural network at the fusion center, and the actual signal direction is used as the label. We model the DOA estimation problem as a multi-label classification one, and the neural network is trained to learn highly nonlinear relationship between the input and the label without knowing their explicit mathematical relationship. Also, the neural networks do not make any assumptions related to the array geometry and their calibration status.

Notations: We use lower-case (upper-case) bold characters to describe vectors (matrices). In particular, $(\cdot)^{\mathrm{T}}$ and $(\cdot)^{\mathrm{H}}$ respectively denote the transpose and conjugate transpose of a matrix or vector. diag$(\cdot)$ denotes a diagonal matrix with the elements of a vector constituting the diagonal entries. triu$(\cdot)$ denotes the upper triangular elements of a matrix. vec$(\cdot)$ denotes vectorizing of a matrix. $\mathbb{E}(\cdot)$ denotes the expectation operation. $\circ$ is the Hadamard product operator. $\jmath = \sqrt{-1}$ denotes the unit imaginary number. $\boldsymbol{I}_M$ stands for the $M \times M$ identity matrix. In addition, $\mathcal{R}(\cdot)$ and $\mathcal{I}(\cdot)$ denote the real part and imaginary part, respectively.

II. Signal Model

Consider an array system with K distributed subarrays, each consisting of M sensors. The distance between the first sensor and the m-th sensor in the k-th subarray is denoted by d_{km} for $k = 1, 2, \cdots, K$ and $m = 1, 2, \cdots, M$. It is assumed that the sensors in each array are located on a half-wavelength grid, i.e., d_{km} are integer multiples of $d = \lambda/2$, where λ denotes the signal wavelength.

A. Subarray Signal Model

P narrowband uncorrelated sources impinge from DOAs $\boldsymbol{\theta} = [\theta_1, \theta_2, \cdots, \theta_P]^{\mathrm{T}}$. The signals waveform of these signals are denoted as $s_p(t)$ for $t = 1, \cdots T$ and $p = 1, \cdots P$. Then, the data vector received at the output of each subarray is expressed as

$$\begin{aligned} \boldsymbol{x}_k(t) &= \sum_{p=1}^{P} \rho_k \boldsymbol{a}_k(\theta_p) s_p(t) + \boldsymbol{n}_k(t) \\ &= \rho_k \boldsymbol{A}_k \boldsymbol{s}(t) + \boldsymbol{n}_k(t), \end{aligned} \tag{1}$$

where ρ_k denotes the phase shift at the reference sensor of the k-th subarray due to the physical location displacement,

$$\boldsymbol{a}_k(\theta_p) = [1, e^{-\jmath \frac{2\pi d_{k2}}{\lambda} \sin(\theta_p)}, \cdots e^{-\jmath \frac{2\pi d_{kM}}{\lambda} \sin(\theta_p)}]^{\mathrm{T}} \tag{2}$$

denotes the steering vector of the k-th subarray for the signal arriving at angle θ_p, λ is the wavelength, and

$$\bar{\boldsymbol{A}}_k = [\boldsymbol{a}_k(\theta_1), \boldsymbol{a}_k(\theta_2), \cdots, \boldsymbol{a}_k(\theta_P)] \tag{3}$$

is the array manifold matrix of the k-th subarray corresponding to the P impinging signals. In addition, the noise vector $\boldsymbol{n}_k(t)$ is assumed to be independent and identically distributed white complex Gaussian entries and are uncorrelated with signals $\boldsymbol{s}(t)$.

When an array sensor has calibration error described by gain and phase errors $\alpha_{k,m} e^{\jmath \beta_{k,m}}$ for $k = 1, \cdots, K$ and $m = 1, \cdots, M$. Denote $\mathbf{g}_k = [\alpha_{k,1} e^{\jmath \beta_{k,1}}, \cdots, \alpha_{k,M} e^{\jmath \beta_{k,M}}]^{\mathrm{T}}$, the actual array manifold $\boldsymbol{A}_k$ becomes

$$\boldsymbol{A}_k = \mathrm{diag}(\mathbf{g}_k) \bar{\boldsymbol{A}}_k. \tag{4}$$

The covariance matrix of the output data vector for the k-th subarray is given as

$$\begin{aligned} \boldsymbol{R}_k &= \mathbb{E}[\boldsymbol{x}_k(t) \boldsymbol{x}_k^{\mathrm{H}}(t)] = \mathbf{A}_k \mathbf{S} \mathbf{A}_k^{\mathrm{H}} + \sigma_{\mathrm{n},k}^2 \mathbf{I}_M \\ &= \sum_{p=1}^{P} \sigma_p^2 \mathbf{a}_k(\theta_p) \mathbf{a}_k^{\mathrm{H}}(\theta_p) + \sigma_{\mathrm{n},k}^2 \mathbf{I}_M, \end{aligned} \tag{5}$$

for $k = 1, \cdots, K$, where $\sigma_{\mathrm{n},k}^2$ denotes the noise power at the k-th subarray and $\mathbf{S} = \mathbb{E}[\mathbf{s}(t) \mathbf{s}^{\mathrm{H}}(t)] = \mathrm{diag}([\sigma_1^2, \sigma_2^2, \cdots, \sigma_P^2])$ is the source covariance matrix with σ_p^2 denoting the power of the p-th source for $p = 1, \cdots, P$. The covariance matrix of the kth subarray is estimated from the sampled data, given as:

$$\hat{\boldsymbol{R}}_k = \frac{1}{T} \sum_{t=1}^{T} \boldsymbol{x}_k(t) \boldsymbol{x}_k^{\mathrm{H}}(t), \tag{6}$$

where T is the number of snapshots.

B. Fusion of the Covariance Matrices

The covariance matrices computed locally at each subarray are transmitted to the fusion center, where further processing is carried out to obtain the total covariance matrix of the system and perform DOA estimation. The aperture of each covariance matrix are different when each array has a different array configuration. In this case, the size of the fused covariance matrices at the fusion center is equal to that of of the largest subarray and is denoted as $L_0 \times L_0$.

The fusion center performs the processing with the received K sets of covariance matrices as described below.

We first define a binary vector $\boldsymbol{c}_k$ to indicate whether a sensor at position ld is present in the kth subarray $\mathbb{S}_k$, i.e.,

$$\langle \boldsymbol{c}_k \rangle_l = \begin{cases} 1, & ld \in \mathbb{S}_k, \\ 0, & \text{otherwise.} \end{cases} \tag{7}$$

where l is the index of the sensor location with $l \in [0, \cdots, L_0]$ and $\langle \cdot \rangle_l$ denotes the element corresponding to the sensor position at ld. We also define $\boldsymbol{C}_k = \boldsymbol{c}_k (\boldsymbol{c}_k)^{\mathrm{T}}$ as the binary mask matrix with unit-valued entries representing observed elements in $\hat{\boldsymbol{R}}_k$.

The total synthesized covariance matrix corresponding to the K subarrays are given as,

$$\boldsymbol{R} = \left(\sum_{k=1}^{K} \hat{\boldsymbol{R}}_k \circ \boldsymbol{C}_k \right) \circ \boldsymbol{D}, \tag{8}$$

where matrix $\boldsymbol{D}$ averages the redundant lag entries in $\hat{\boldsymbol{R}}_k$. The (u, v)th element of matrix $\boldsymbol{D}$ is given as

$$[\boldsymbol{D}]_{u,v} = \frac{1}{\sum_{i=1}^{K} [\boldsymbol{C}]_{u,v} + \epsilon}, \tag{9}$$

with ϵ denoting a small positive value in order to provide stability of the division.

Because matrix $\boldsymbol{R}$ is Hermitian, we only use the upper triangular elements which include all the necessary information. The upper triangular elements are vectorized as

$$\bar{\boldsymbol{r}} = \mathrm{vec}(\mathrm{triu}(\boldsymbol{R})), \tag{10}$$

where $R_{l_1 l_2}$ is the (l_1, l_2)-th element of the covariance matrix $\boldsymbol{R}$. The real and imaginary parts are separated to form the following real-valued vector,

$$\boldsymbol{r} = [(\mathcal{R}(\bar{\boldsymbol{r}}))^{\mathrm{T}} \ (\mathcal{I}(\bar{\boldsymbol{r}}))^{\mathrm{T}}]^{\mathrm{T}}. \tag{11}$$

Fig. 1: Proposed neural network structure.

III. Neural Network-Based DOA Estimation

In this section, we describe the the proposed neural network-based DOA estimation procedure. Vector $\boldsymbol{r}$ is applied to the input node of the neural network, and true signal DOAs are used as the the label. The neural network learn the nonlinear relationship between the input and label by minimizing a predefined cost function.

The proposed fully connected neural network is shown in Fig. 1, where 2 hidden layers are used. The number of hidden layer traded off between the nonlinear expressivity of the model and its overfitting risk. The network can improve the nonlinear mapping between input and the label with its depth, but it in turns raises the complexity and thus overfitting. Each unit in a hidden layer performs logistic regression operation. A nonlinear activation function is applied on the logistic regression output.

When there are $N > 1$ observations, the complete input dataset $\boldsymbol{X}$ is formed by concatenating vectors $\boldsymbol{r}_1, \cdots, \boldsymbol{r}_N$, expressed as

$$\boldsymbol{X} = [\boldsymbol{r}_1, \boldsymbol{r}_2, \cdots, \boldsymbol{r}_N]. \tag{12}$$

Denote $\boldsymbol{Z}^{[d]}$, $f^{[d]}$, and $\boldsymbol{\mathcal{A}}^{[d]}$ as the logistic regression output, activation function, and the activation resulted from nonlinear activation function from the d-th hidden layer, respectively, for $d = 1, 2, 3$. Denote also $\boldsymbol{W}^{[d]}$ and $b^{[d]}$ as the weights and biases corresponding to the d-th hidden layer. Then, the outputs from the d-th hidden layer is expressed as,

$$\begin{aligned} \boldsymbol{Z}^{[d]} &= \boldsymbol{W}^{[d]}\boldsymbol{\mathcal{A}}^{[d-1]} + b^{[d]}, \\ \boldsymbol{\mathcal{A}}^{[d]} &= f^{[d]}(\boldsymbol{Z}^{[d]}). \end{aligned} \tag{13}$$

For the first hidden layer, the activation from the previous layer is the input, i.e., $\boldsymbol{\mathcal{A}}^{[d-1]} = \boldsymbol{X}$. For activation function $f^{[d]}$, we use the rectified linear Unit (ReLU) activation function in the hidden layers. The ReLU activation function is chosen because it makes the computation faster compared to other activation functions such as sigmoid and tanh, as its slope does not diminsh to 0. Since we consider the DOA estimation problem as a binary classification problem, we use sigmoid activation function for the output layer, which converts the values form the output node between 0 to 1.

A binary cross entropy loss function is used for the underlying binary classification problem. The gradient descent algorithm is used to minimize the cost function. Hence, our optimization problem becomes optimizing the weights $\boldsymbol{W}$ and biases $\boldsymbol{b}$ to minimize the overall cost function, expressed as

$$\min_{\boldsymbol{W},\boldsymbol{b}} -\frac{1}{J}\sum_{i=1}^{J}\left[\boldsymbol{Y}_j^{[i]}\log\hat{\boldsymbol{Y}}_j^{[i]} + \left(1-\boldsymbol{Y}_j^{[i]}\right)\log\left(1-\hat{\boldsymbol{Y}}_j^{[i]}\right)\right], \tag{14}$$

where J is the number of training samples in the j-th minibatch of the training data, and $\hat{\boldsymbol{Y}}_j^{[i]}$ and $\boldsymbol{Y}_j^{[i]}$ are the predicted output and the actual label of the i-th sample at the j-th minibatch of the neural network, respectively. The cost function is computed for each of the training examples and the weights of the model are updated only when the training process of all of the examples of this particular minibatch is completed.

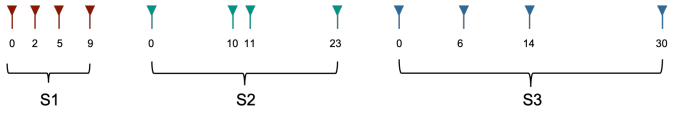

Fig. 2: Array configuration.

IV. Experimental results

In this section, we present experimental results which compare the results from our neural network approach with the MUSIC algorithm developed using matrix interpolation.

A. Simulation Settings

We consider a distributed array system with 3 spatially distributed platforms placed in a collinear fashion. Each array consists of 4 sensors. As such, we use a total of 12 sensors in the system placed in these distributed subarrays. The array configuration is depicted in Fig. 2 where the numbers indicate the relative sensor position in each subarray with a unit of half wavelength. That is, the sensor locations for each subarray are given as:

$$\begin{aligned} \mathbb{S}_1 &= \{0, 2, 5, 9\}\lambda/2, \\ \mathbb{S}_2 &= \{0, 10, 11, 23\}\lambda/2, \\ \mathbb{S}_3 &= \{0, 6, 14, 30\}\lambda/2. \end{aligned} \tag{15}$$

As we consider non-coherent process with partly calibrated array, we have the knowledge of the relative sensor positions within each subarray, but we do not know the exact distance between the subarrays. The largest aperture of these subarray is $L_0 = 31$. Note that, in this example, each subarray is sparse. Therefore, the 31×31 fused covariance matrix computed at the fusion center is also sparse with missing entries.

We generate our training dataset by considering the signals impinging from directions within the range of $[-60°, 60°]$. The entire spatial space is discretized with a $1°$-interval, rendering 121 direction grids. We consider $K = 15$ sources with varying angular separation $\Delta\phi$ to be $1°$, $2°$, $3°$, and $4°$. For each angular separation $\Delta\phi$, the direction of the first signal θ_0 is randomly chosen with a uniform probability within the range of $\theta = [-60°, 60° - \Delta\phi]$, and the DOA of the n-th signal ($n \geq 2$) is $\theta_0 + (n-1)\Delta\phi$. The input signal-to-noise ratio (SNR) is set to 0 dB. The antenna gains are independently generated from a uniform distribution between 0.9 and 1.1, whereas the phase errors are indepdently generated from a uniform distribution between $-9°$ and 9 degree.

For a given direction, 20 groups of snapshots are generated with random noises. We generate a total number of $3,040$ data vectors in our training dataset. 90% of them are used for training and the other 10% are used for validation. These vectors are used as the training input of the neural network. For the label of the neural network, the true signal direction is used.

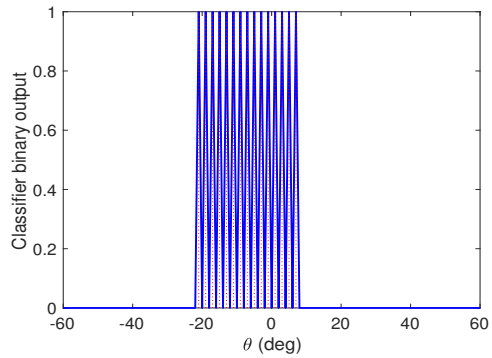

(a) Neural network output label

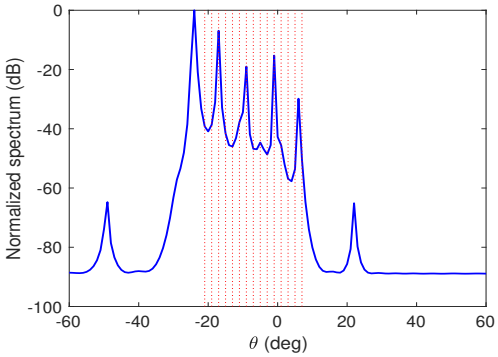

(b) MUSIC pseudo-spectrum

Fig. 3: Comparison between the output label of the proposed method and the MUSIC pseudo-spectrum.

For example, in the case of $\theta_0 = -60^\circ$ and $\Delta\phi = 1^\circ$, when there are two signals impinging from the direction -59° and -57°, respectively, the label will be $[0, 1, 0, 1, 0, 0, 0, \cdots, 0]$. In this multi-label binary classification scheme, the output we obtain from the network is a 121×1 binary vector. We use the Adam optimizer to optimize the weights of the network which minimize the cost function, and the learning rate is set to 0.001. The minibatch size is set to $J = 64$ and 500 epochs are used to train the network.

B. DOA Estimation Performance

The performance comparison of the proposed machine learning approach with conventional MUSIC algorithm is illustrated in Fig. 3. For MUSIC, covariance matrix interpolated using structured matrix completion [31, 32] is employed. Because of the high number of closely located sources and the array sensor calibration errors, the covariance matrix interpolation does not work well. As a result, as shown in Fig. 3(b), the MUSIC algorithm does not offer resolved spatial spectrum. In contrast, the performance of the proposed neural network-based method produces accurate DOA estimation results. Fig. 3(a) shows the estimated binary classification results with value "1" indicates the existence of a signal in that direction.

V. CONCLUSION

In this paper, we considered robust DOA estimation in a distributed array platform. We considered non-coherent data processing at the fusion center, where covariance matrices form each of the individual subarrays are combined. To obtain the direction of arrivals of the impinging signals from the fused covariance matrix, we propose a neural network-based DOA estimation method. This method is capable of resolving the DOAs of a high number of closely located sources and is immune to array calibration errors. The effectiveness and robustness of the proposed technique were verified through simulation results.

VI. REFERENCES

[1] D. H. Johnson and D. E. Dudgeon, *Array Signal Processing: Concepts and Techniques*. Simon & Schuster, 1992.

[2] H. L. Van Trees, *Optimum Array Processing: Part IV of Detection, Estimation, and Modulation Theory*. Wiley, 2002.

[3] T. E. Tuncer and B. Friedlander (Eds.), *Classical and Modern Direction-of-Arrival Estimation.* Elsevier, 2009.

[4] B. D. Van Veen and K. M. Buckley, "Beamforming: A versatile approach to spatial filtering," *IEEE ASSP Mag.*, vol. 5, no. 2, pp. 4–24, Apr. 1988.

[5] J. Litva and T. K. Lo, *Digital Beamforming in Wireless Communications.* Artech House, 1996.

[6] J. Li and P. Stoica, *Robust Adaptive Beamforming*. Wiley, 2005.

[7] R. O. Schmidt, "Multiple emitter location and signal parameter estimation," *IEEE Trans. Antennas Propag.*, vol. AP-34, no. 3, pp. 276–280, Mar. 1986.

[8] R. Roy and T. Kailath, "ESPRIT–Estimation of signal parameters via rotational invariance techniques," *IEEE Trans. Acoust., Speech, Signal Process.*, vol. 37, no. 7, pp. 984–995, July 1989.

[9] D. Malioutov, M. Çetin, and A. S. Willsky, "A sparse signal reconstruction perspective for source localization with sensor arrays," *IEEE Trans. Signal Process.*, vol. 53, no. 8, pp. 3010–3022, Aug. 2005.

[10] Z.-M. Liu, Z.-T. Huang, and Y.-Y. Zhou, "An efficient maximum likelihood method for direction-of-arrival estimation via sparse Bayesian learning," *IEEE Trans. Wireless Commun.,* vol. 11, no. 10, pp. 1–11, Oct. 2012.

[11] Z. Yang, L. Xie, and C. Zhang, "Off-grid direction of arrival estimation using sparse Bayesian inference," *IEEE Trans. Signal Process.*, vol. 61, no. 1, pp. 38–43, Jan. 2013.

[12] Y. D. Zhang, M. G. Amin, and B. Himed, "Sparsity-based DOA estimation using co-prime arrays," in *Proc. IEEE Int. Conf. Acousti., Speech, Signal Process. (ICASSP)*, Vancouver, Canada, May 2013.

[13] S. Qin, Y. D. Zhang, and M. G. Amin, "Generalized coprime array configurations for direction-of-arrival estimation," *IEEE Trans. Signal Process.*, vol. 63, no. 6, pp. 1377–1390, March 2015.

[14] C. Zhou, Y. Gu, Y. D. Zhang, Z. Shi, T. Jin, and X. Wu, "Compressive sensing based coprime array direction-of-arrival estimation," *IET Commun.*, vol. 11, no. 11, pp. 1719–1724, Aug. 2017.

[15] Z.-M. Liu and F.-C. Guo, "Azimuth and elevation estimation with rotating long-baseline interferometers," *IEEE Trans. Signal Process.*, vol. 63, no. 9, pp. 2405-2419, May 2015.

[16] M. Guo, Y. D. Zhang, and T. Chen, "DOA estimation using compressed sparse array," *IEEE Trans. Signal Process.*, vol. 66, no. 15, pp. 4133–4146, Aug. 2018.

[17] A. Moffet, "Minimum-redundancy linear arrays," *IEEE Trans. Antennas Propagat.*, vol. 16, no. 2, pp. 172–175, March 1968.

[18] E. Vertatschitsch and S. Haykin, "Nonredundant arrays," *Proc. IEEE*, vol. 74, no. 1, pp. 217–217, Jan. 1986.

[19] R. T. Hoctor and S. A. Kassam, "The unifying role of the

co-array in aperture synthesis for coherent and incoherent imaging," *Proc. IEEE*, vol. 78, no. 4, pp. 735–752, April 1990.

[20] D. A. Linebarger, I. H. Sudborough, and I. G. Tollis, "Difference bases and sparse sensor arrays," *IEEE Trans. Inf. Theory*, vol. 39, no. 2, pp. 716–721, Mar. 1993.

[21] P. Pal and P. P. Vaidyanathan, "Nested arrays: A novel approach to array processing with enhanced degrees of freedom," *IEEE Trans. Signal Process.,* vol. 58, no. 8, pp. 4167–4181, Aug. 2010.

[22] P. P. Vaidyanathan and P. Pal, "Sparse sensing with co-prime samplers and arrays," *IEEE Trans. Signal Process.,* vol. 59, no. 2, pp. 573–586, Feb. 2011.

[23] J. Liu, Y. Zhang, Y. Lu, S. Ren, and S. Cao, "Augmented nested arrays with enhanced DOF and reduced mutual coupling," *IEEE Trans. Signal Process.*, vol. 65, no. 21, pp. 5549–5563, Nov. 2017.

[24] Z. Zheng, W.-Q. Wang, Y. Kong, and Y. D. Zhang, "MISC array: A new sparse array design achieving increased degrees of freedom and reduced mutual coupling effect," *IEEE Trans. Signal Process.*, vol. 67, no. 7, pp. 1728–1741, Apr. 2019.

[25] S. Ren, W. Dong, X. Li, W. Wang, and X. Li, "Extended nested arrays for consecutive virtual aperture enhancement," *IEEE Signal Process. Lett.*, vol. 27, pp. 575–579, Mar. 2020.

[26] R. Cohen and Y. C. Eldar, "Sparse array design via fractal geometries," *IEEE Trans. Signal Process.*, vol. 68, no. 7, pp. 4797–4812, Aug. 2020.

[27] A. Ahmed and Y. D. Zhang, "Generalized non-redundant sparse array designs," *IEEE Trans. Signal Process.*, vol. 69, pp. 4580–4594, Aug. 2021.

[28] W. Suleiman, P. Parvazi, M. Pesavento, and A. M. Zoubir, "Non-coherent direction-of-arrival estimation using partly calibrated arrays," *IEEE Trans. Signal Process.*, vol. 66, no. 21, pp. 5776–5788, Nov. 2018.

[29] B.-X. Chen, G.-H. Chen, and M.-L. Yang, "High accuracy 2-D angle estimation using distributed coherent arrays," *J. Electron. Inform. Tech.* vol. 34, no. 11, pp. 2621–2627, 2012.

[30] Y. Liao, R. Zhao and H. Liu, "DOA estimation method with the distributed nested array," in *2018 10th Int. Conf. Wireless Commun. Signal Process. (WCSP)*, pp. 1–6. 2018.

[31] C. Zhou, Y. Gu, X. Fan, Z. Shi, G. Mao, and Y. D. Zhang, "Direction-of-arrival estimation for coprime array via virtual array interpolation," *IEEE Trans. Signal Process.*, vol. 66, no. 22, pp. 5956–5971, Nov. 2018.

[32] S. Zhang, A. Ahmed, Y. D. Zhang, and S. Sun, "Enhanced DOA estimation exploiting multi-frequency sparse array," *IEEE Trans. Signal Process.*, vol. 69, pp. 5935–5946, 2021.

[33] G. Hinton *et al.*, "Deep neural networks for acoustic modeling in speech recognition: The shared views of four research groups," *IEEE Signal Process. Mag.*, vol. 29, no. 6, pp. 82–97, Nov. 2012.

[34] L. Zhang, F. Yang, Y. D. Zhang, and Y. J. Zhu, "Road crack detection with deep convolution neural network," in *Proc. IEEE Int. Conf. Image Process. (ICIP)*, Phoenix, AZ, Sept. 2016.

[35] P. Kuang, T. Ma, Z. Chen, and F. Li, "Image super-resolution with densely connected convolutional networks," *Appl. Intell.*, vol.49, pp.125–136, 2019.

[36] H. Xian, B. Chen, T. Yang, D. Liu, "Phase enhancement model based on supervised convolutional neural network for coherent DOA estimation," *Appl. Intell.*, vol. 50, pp. 2411–2422, 2020.

[37] M. Pastorino and A. Randazzo, "A smart antenna system for direction of arrival estimation based on a support vector regression," *IEEE Trans. Antennas Propag.*, vol. 53, no. 7, pp. 2161–2168, July 2005.

[38] A. Randazzo, M. A. Abou-Khousa, M. Pastorino, and R. Zoughi, "Direction of arrival estimation based on support vector regression: Experimental validation and comparison with MUSIC," *IEEE Antennas Wireless Propag. Lett.*, vol. 6, pp. 379–382, 2007.

[39] A. Rawat, R. N. Yadav, and S. Shrivastava, "Neural network applications in smart antenna arrays: A review," *AEU-Int. J. Electron. Commun.*, vol. 66, no. 11, pp. 903–912, Nov. 2012.

[40] K. Terabayashi, R. Natsuaki, and A. Hirose, "Ultrawideband direction-of-arrival estimation using complex-valued spatiotemporal neural networks," *IEEE Trans. Neural Netw. Learn. Syst.*, vol. 25, no. 9, pp. 1727–1732, Sep. 2014.

[41] Y. Gao, D. Hu, Y. Chen, and Y. Ma, "Gridless 1-b DOA estimation exploiting SVM approach," *IEEE Commun. Lett.*, vol. 21, no. 10, pp. 2210–2213, Oct. 2017.

[42] L. Wu, Z. Liu, and Z. Huang, "Deep convolution network for direction of arrival estimation with sparse prior," *IEEE Signal Process. Lett.*, vol. 26, no. 11, pp. 1688–1692, Nov. 2019.

[43] Z. Liu, C. Zhang, and P. S. Yu, "Direction-of-arrival estimation based on deep neural networks with robustness to array imperfections," *IEEE Trans. Antennas Propag.*, vol. 66, no. 12, pp. 7315–7327, Dec. 2018.

[44] H. Xiang, B. Chen, M. Yang, S. Xu, and Z. Li, "Improved direction-of-arrival estimation method based on LSTM neural networks with robustness to array imperfections," *Appl. Intell.*, vol. 51, pp. 4420–4433, 2021.